Published in final edited form as:
Proteins. 2009 April ; 75(1): 111–117. doi:10.1002/prot.22225.

Molecular Basis For Dimer Formation of TRβ Variant D355R

Natalia Jouravel[a], **Elena Sablin**[a], **Marie Togashi**[b], **John D. Baxter**[b], **Paul Webb**[b], and **Robert J. Fletterick**[a]

[a]Department Biochemistry and Biophysics, University of California, San Francisco, 600 16th Street, Genentech Hall, San Francisco, CA 94158, USA. Tel: 415-476-5051; Fax: 415-476-1902; email: njouravel@msg.ucsf.edu / sablin@msg.ucsf.edu / flett@msg.ucsf.edu

[b]Diabetes Center & Dept. of Medicine, University California San Francisco (UCSF), 513 Parnassus Avenue, S-1222, Box 0540, Medical Sciences Building, San Francisco, CA 94143, USA. Tel: 415-476-6789; Fax: 415-564-5813; email: mtogashi@diabetes.ucsf.edu / JBaxter918@aol.com / pwebb@diabetes.ucsf.edu

Abstract

Protein quality and stability are critical during protein purification for X-ray crystallography. A target protein that is easy to manipulate and crystallize becomes a valuable product useful for high throughput crystallography for drug design and discovery. In this work, a single surface mutation, D355R, was shown to be crucial for converting the modestly stable monomeric ligand binding domain of the human thyroid hormone receptor (TR LBD) into a stable dimer. The structure of D335R TR LBD mutant was solved using X-ray crystallography and refined to 2.2 Å resolution with Rfree/R values of 24.5/21.7. The crystal asymmetric unit reveals the TR dimer with two molecules of the hormone-bound LBD related by a two-fold symmetry. The ionic interface between the two LBDs comprises residues within loop H10-H11 and loop H6-H7 as well as the C-terminal halves of helices 8 of both protomers. Direct intermolecular contacts formed between the introduced residue Arg 355 of one TR molecule and Glu 324 of the second molecule become a part of the extended dimerization interface of 1330 $Å^2$ characteristic for a strong complex assembly that is additionally strengthened by buffer solutes.

Keywords

thyroid hormone receptor; ligand binding domain; homodimer; protein purification; crystal structure

1. Introduction

Thyroid hormone receptor (TR) belongs to the family of nuclear transcriptional regulators, proteins intensively studied for development of new pharmaceuticals (1,2). TR is a drug target for diabetes, obesity and other thyroid dysfunctions as it regulates numerous metabolic processes through transcriptional control of its target genes. TR is required for normal function of nearly all tissues and organs, and it is vital for regulation of oxygen consumption and metabolic rate. Multiple functions of TR are explained in part by its ability to form homodimers or heterodimers with retinoid X receptor (RXR) (3,4). The dimerization event is controlled by different ligands in different cellular contexts or may not require ligands for either receptor (5,6). Additional diversity in function comes from four existing TR isoforms that are products of two distinct genes and alternate splicing (7). The $TR\alpha_1$, $TR\beta_1$ and $TR\beta_2$ isoforms are expressed in most tissues; they bind thyroid hormones and function as ligand-regulated transcription factors. In contrast, the $TR\alpha_2$ isoform does not

bind hormone and is prevalent in pituitary and central nervous system (8,9). Selective targeting of the tissue specific TR isoforms is a major goal of drug development.

Similar to other nuclear receptors (NRs), TR has a modular structure consisting of a ligand-independent N-terminal domain (AF1), which associates with transcriptional regulators, a highly conserved DNA-binding domain (DBD), and a C-terminal ligand-binding domain (LBD) (9). TR LBD mediates transcriptional activation or repression through conformational changes induced by hormone binding (10,11). Several structures of TRα and TRβ LBD bound by activating ligands have been determined to date, all of which are of the TR monomer in the stable agonist-bound conformation (12,13). Similar to other NRs, the TR LBD comprises a three-layered sandwich structure formed by 12 α-helices and two short β-strands. The bound ligand agonist completes the hydrophobic core of the LBD.

For rational design of TR specific drugs, high-resolution structural data revealing the molecular basis of ligand selectivity are particularly useful (2,14). However, the TR LBD has proven to be a delicate protein and a challenging crystallization target. For difficult to crystallize proteins, improving protein behavior through protein engineering has shown good results. The most common approaches include mutating surface cysteine residues (15) or removing unstructured loops or hinge regions (16) that might cause structural heterogeneity. One report described a rational possibility of improving crystallizability of proteins through designing symmetrical covalent oligomers stabilized by synthetic Cys-Cys contacts (17). Our study demonstrates a unique approach when the monomeric protein has been stabilized via formation of a symmetrical non-covalent homodimer. This designed homodimer is characterized by an extended dimerization interface built by combination of physical forces: hydrophobic interactions, hydrogen bonds and electrostatic contacts.

2. Experimental procedures

2.1. Protein expression and purification

A cDNA fragment encoding human TRβ LBD (a.a. 209-461) was made using PCR and cloned into pETDuet-1 expression vector (Novagen) using BamHI/HindIII restriction sites. The D355R mutation was introduced using QuickChange kit (Stratagene) according to the manufacturer's protocol. The resulting recombinant plasmid was verified by sequencing. The recombinant His_6-tagged D355R TRβ LBD was expressed in *E. coli* BL21(DE3) host (Invitrogen). Cells were grown at 37°C in LB medium supplemented with 100 μg/ml ampicillin until OD_{600}~0.6. Expression was induced by addition of isopropyl-β-thiogalactoside (IPTG) to a final concentration of 0.5 μM, cells were grown for 12 hours at 15° C and harvested by centrifugation at 5,000 g for 15 min. The cell pellets from 1 L of culture were resuspended in 20 ml of buffer A (20 mM Tris-HCl pH 8, 300 mM NaCl, 50mM lithium sulfate, 25 mM imidazole, 3mM β-OG, 0.2 mM PMSF, 10% glycerol, 200 μg/ml lysozyme, 30 μM TRIAC), cells were lysed by sonication, and cell lysates centrifuged at 15,000 g for 30 min at 4°C. The supernatant was loaded onto a 5 ml Ni^{2+}-affinity column (HiTrap chelating column, Amersham Biosciences) equilibrated with buffer A using the Äkta FPLC system (Amersham Biosciences). The column was washed with 20 volumes of buffer A. Bound proteins were eluted with buffer A containing 500 mM imidazole. Fractions containing eluted proteins were pooled and dialysed overnight against buffer B (10 mM Tris-HCl pH 7.5, 150 mM NaCl, 50mM lithium sulfate, 10% glycerol, 5 mM DTT, 1mM EDTA) with two fold molar excess of TRIAC (Sigma). The protein was then further purified using a Superdex 75 16/60 size exclusion column (Amersham Biosciences) calibrated with globular standard proteins (gel-filtration calibration kit, Amersham Biosciences) and equilibrated with buffer B. The protein eluted in two distinct fractions corresponding to the TR homodimer and monomer. The main protein fraction corresponding to the TR

homodimer (~80% of total protein) was concentrated and rechromatographed using the same size exclusion column.

2.2. Crystallization

The purified TRβ was concentrated to ~ 20 mg/ml, incubated with a two fold molar excess of TRIAC, and centrifuged for 20 min at 14,000 g prior to crystallization. Crystallization trials were performed by the hanging-drop vapor diffusion method at 17 °C using 24-well plates (Qiagen). Different commercial crystallization screens (Hampton Research, Emerald BioSystems, Qiagen) were used to determine the initial crystallization conditions. The protein solution (1 μl) was mixed with an equal volume of the reservoir solution and placed on the cover slips over the well containing 1 ml of reservoir solution. Several high ionic strength conditions containing ammonium sulfate (1.5 - 2 M) or sodium citrate (1.4 - 1.6 M) produced small needle-like crystals. The largest cluster of crystals was grown using 25% ethylene glycol as precipitant (condition No. 3, Crystal Screen 2, Hampton Research). These crystals appeared within 3-5 days and grew to their full size within a week at room temperature. The cluster was made of large thin blades that were separated into individual crystals of ~ 550 × 400 × 10 μm. These individual crystals were used for data collection.

Clustered crystals were reproducibly grown from either freshly prepared or frozen protein. Comparable quality data sets were collected using crystals obtained from either preparation.

2.3. Data collection and processing

Protein crystals were mounted directly from the drop containing mother liquor into cryo loops (Hampton Research) and flash-frozen in liquid nitrogen. X-ray diffraction data were measured at −180 °C and collected to 2.2 Å at the Advanced Light Source (Lawrence Berkeley National Laboratory) Beamline 8.3.1 (λ= 1.1 Å) using a single crystal. The crystal was rotated through 180° with an oscillation angle of 1° per frame and an exposure time of 3 s per image. Diffraction data were processed using DENZO and scaled with SCALEPACK (18). The crystal was of the monoclinic space group $P2_1$, with one homodimer in the asymmetric unit and cell dimensions of a=55.6 Å, b=93.0 Å, c=58.8 Å, and $\beta=110.0^0$. The solvent content of the crystal was ~46.3%, with Matthew's coefficient of ~2.4 $Å^3$/Da.

The structure of the TR homodimer was determined by the molecular replacement method using the program package CNS and the structure of TRβ LBD (PDB ID 1NAX) as a search model. All water and ligand molecules as well as the C-terminal helix H12, which could adopt different conformations depending on the presence of a ligand, were removed from the search model. The cross-rotation search algorithm implemented in the CNS package produced two independent solutions, consistent with the presence of two LBDs in the asymmetric unit. The final solution for the LBD dimer had a monitor value of 0.555 and a packing coefficient of 0.45. The presence of a clear electron density for the two TRIAC molecules in the difference Fourier (Fo-Fc) maps for the protein model confirmed the molecular replacement solution. Additionally, the presence of continuous and well-defined electron density for helices H12 in the expected agonist position became apparent at the early stages of the structure refinement. The tetrahedrally shaped density observed at the dimer interface was attributed unambiguously to SO^{4-} ion, due to the presence of sulfate in the buffer solutions.

The current model for the TRβ homodimer is refined to 2.2 Å resolution with Rfree/R values of 24.5/21.7 and contains 494 amino acid residues, 2 TRIAC molecules, 1 sulfate ion and 123 water molecules. Analysis of the stereochemistry of the model using PROCHECK (19) indicates that the main chain dihedral angles for all residues are located in the permitted regions of the Ramachandran diagram and that the root mean square deviations from ideal

values are distributed within the expected range for a well refined structure. Data collection and refinement statistics are summarized in Table I. The structure has been deposited with the Protein Data Bank (PDB) and assigned the following ID Number: RCSB ID code rcsb047606 and PDB ID code 3D57.

Results and Discussion

In our experience, TR LBD is a delicate protein that crystallizes only when carefully prepared fresh. Because of the protein instability, TR requires many iterative protein preparations for obtaining and optimizing crystals suitable for high-resolution structural analysis. In addition, TR is unstable without a ligand, which is absolutely required during protein purification at all stages. When stabilized by a bound ligand, TR LBD is a monomer in solution, although it is shown to form dimers and trimers on DNA *in vivo* (4,20). To date, there is no crystal structure of any TR self-assembly, however extensive mutational analyses and homology modeling suggested that TR LBD might employ helix 11 to form dimers (21). Independent studies showed that clustered charged surface residues in helices 7 and 8 might influence stability of the TR LBD and affect its dimerization on DNA and function on TR response elements (22). In particular, a single surface mutation D355R in helix 8 was shown to enhance TR homodimer formation on DNA in the presence of hormone (22). This observation was noteworthy because it revealed a curious improvement of protein stability without any obvious explanation. This mutation is remote from the predicted dimerization helix 11, therefore, the molecular mechanism of the assembly enhancement could not be explained by similarities with other NR homodimers (23,24,25).

Any novel protein assemblies provide useful information of higher order complex architecture (26). Moreover, homodimeric complexes are generally more stable and, therefore, amenable for protein crystallization (17,27). In this work, we performed a detailed structural and functional analysis of D355R TR LBD and its dimeric assembly. Specifically, we determined the three-dimensional structure of this protein to visualize the mechanism of its dimerization. We complemented this structural study with analyses of the protein stability, behavior in solution and ultimately its utility for high throughput crystallographic techniques.

We found that in contrast to the wild type TR monomer, the mutant receptor LBD undergoes a ligand-dependent molecular assembly, forming a homodimer in addition to the monomer in certain preparative conditions. In our experiments, a typical size exclusion chromatography run for the purified D355R TR mutant protein resulted in separation of 60 kDa from 30kDa protein species, which correspond to the dimeric and monomeric states of TR LBD (Fig. 1A). Repeated chromatography of the main protein fraction corresponding to the TR homodimer (~80% of total protein) demonstrated that the formed dimer is stable under the experimental conditions (Fig. 1A). Altering the buffer composition such as removal of sulfate ions, resulted in loss of dimers, with only monomeric protein present in the chromatographic fractions (Fig.1B). In contrast, the TR homodimer formed very efficiently if sulfate ions were present in preparative buffers (Fig.1B). Other variations in protein buffers such as ionic strength, pH and the presence of detergents were also found to influence formation of the TR homodimer and the dimer/monomer partition in solution (data not presented). Based on these experiments, we found the protein preparation conditions that allow purification of the TR homodimer as a major protein fraction with high yield (specified in Experimental procedures). The ultimate step of protein purification employing FPLC was critical as it resulted in efficient separation of the dimeric protein from the TR LBD monomer, thus ensuring protein purity and homogeneity. After this final purification step, the TR homodimer was more than 95% pure as judged by gel electrophoresis. Furthermore, the D355R TR dimer was highly soluble and maintained its monodisperse

dimeric state both at high (40mg/ml) and low (5mg/ml) concentrations as judged by native gels and size exclusion chromatography analyses. Notably, the TR LBD retained its dimeric state not only throughout protein preparation, but also after several freeze-thaw cycles, as judged by size exclusion chromatography. Based on these observations, we conclude that the dimeric form of the mutant increased stability of the TR LBD, which could tolerate 2-3 cycles of freezing – thawing and produce high quality crystals that diffracted to 2.0 - 2.5 Å resolution. The increased stability of TR LBD is a crucial improvement as wild type protein could not produce crystals upon storage or freezing. Furthermore, these improved protein and crystal properties are compliant with the demands of a high throughput crystallography (28,29).

The structure of the TR homodimer was determined by the molecular replacement method and refined to 2.2 Å resolution with Rfree/R values of 24.5/21.7. The current model includes residues 210-460 and 211-460 for the first and the second TRIAC bound TR LBDs (Fig. 2A). The unstructured loop residues 255-260 (chain A) and residues 256 and 257 (chain B) are omitted from the model due to the lack of electron density. There are 123 water molecules and one coordinated sulfate ion in the TR homodimer structure. Data collection and refinement statistics are summarized in Table I.

The crystal structure of TR homodimer showed that D355R mutation affected neither the tertiary structure of the nuclear receptor LBD nor its AF-2 surface as judged by comparison of the two LBDs from the complex with available structure of monomeric TR (PDB ID 1NAX). The structure of TR mutant revealed one homodimer in the crystal asymmetric unit (Fig.2). The two monomers in the complex are related by two-fold non-crystallographic symmetry and are structurally very similar to each other, with r.m.s. deviation of only 0.23 Å for 169 Cα atoms. The dimer interface is extensive (~ 1330 $å^2$) and is formed between mostly polar or charged residues (Table II). Hydrogen bonds link the side chains of the interfacial residues through six water molecules that are shared at the interface. Although mostly composed of polar and charged residues, the dimer interface is additionally stabilized by hydrophobic interactions (Table II). The residues forming contacts between monomers are mostly contributed from helix 8 and loops H6-H7 and H10-H11. There are two sites at the interface that are evidently crucial for the dimer formation. The first site includes a four-histidine cluster composed of H412 and H413 from the two TR LBDs. A single sulfate ion links the four His side chains within the cluster; His412 requires a water molecule to bridge to the sulfate ion (Fig.2B). The presence of the coordinated sulfate ion at the dimer interface is consistent with our biochemical data showing the necessity of sulfate for dimerization of the mutant TR LBD (Fig. 1B). The second site is composed of residue R338 and mutated residue R355 of each monomer that form hydrogen bonds to the oppositely charged E324 and E326 of the partner LBD (Fig.2B). In wild type TR, side chain of D355 forms salt bridge with the side chain of R338, which is also hydrogen bonded with the side chain of D351. Thus R338, D351 and D355 are charged residues of a solvated 3 side chain intramolecular cluster. In the dimer, the polar interaction network is intermolecular.

Based on the data described here, we conclude that with the strategically placed single surface mutation D355R we engineered a symmetrical dimer of TR LBD with an interface composed mostly of polar amino acid side chains. The polar side chains are partly solvated, the dimer interface contains 6 water molecules (Fig.2C). The interface has almost no significant hydrophobic interactions, with only 10% of the contacts formed between paired nonpolar atoms.

The mutant TR is characterized by the increased protein stability and crystallizability and thus is a good tool for crystal based screenings employing high throughput soakings of surface binding small molecules. We can envision other nuclear receptors being amenable

for dimer engineering, making this approach a valuable technique for obtaining stable protein tools for high resolution crystallography. Predicting single site mutants that would form stable protein dimers is recognized to be challenging. The results presented here suggest that appropriate stabilizing residues for the protein of interest are better found by experiment with a biochemical assay for stability.

Acknowledgments

We thank James Holton and George Meigs for assistance with data collection at the Advanced Light Source 8.3.1. Beamline (University of California Berkeley).

Funding: project was supported by NIH R01 DK51281 and DK41842 (J. Baxter), and RO1 DK058080 (R. Fletterick and R. Guy).

References

1. Gronemeyer H, Gustafsson JA, Laudet V. Principles for modulation of the nuclear receptor superfamily. Nat Rev Drug Discov. 2004; 3(11):950–64. [PubMed: 15520817]
2. Baxter JD, Dillmann WH, West BL, Huber R, Furlow JD, Fletterick RJ, Webb P, Apriletti JW, Scanlan TS. Selective modulation of thyroid hormone receptor action. J Steroid Biochem Mol Biol. 2001; 76(1-5):31–42. [PubMed: 11384861]
3. Zhang XK, Hoffmann B, Tran PB, Graupner G, Pfahl M. Retinoid X receptor is an auxiliary protein for thyroid hormone and retinoic acid receptors. Nature. 1992; 30;355(6359):441–6. [PubMed: 1310350]
4. Williams GR, Harney JW, Forman BM, Samuels HH, Brent GA. Oligomeric binding of T3 receptor is required for maximal T3 response. J Biol Chem. 1991; 15;266(29):19636–44. [PubMed: 1918070]
5. Li D, Li T, Wang F, Tian H, Samuels HH. Functional evidence for retinoid X receptor (RXR) as a nonsilent partner in the thyroid hormone receptor/RXR heterodimer. Mol Cell Biol. 2002; 22(16): 5782–92. [PubMed: 12138189]
6. Collingwood TN, Butler A, Tone Y, Clifton-Bligh RJ, Parker MG, Chatterjee VK. Thyroid hormone-mediated enhancement of heterodimer formation between thyroid hormone receptor beta and retinoid X receptor. J Biol Chem. 1997; 16;272(20):13060–5. [PubMed: 9148917]
7. Wood WM, Ocran KW, Gordon DF, Ridgway EC. Isolation and characterization of mouse complementary DNAs encoding alpha and beta thyroid hormone receptors from thyrotrope cells: the mouse pituitary-specific beta 2 isoform differs at the amino terminus from the corresponding species from rat pituitary tumor cells. Mol Endocrinol. 1991; 5(8):1049–61. [PubMed: 1944303]
8. Baas D, Bourbeau D, Carre JL, Sarlieve LL, Dussault JH, Puymirat J. Expression of alpha and beta thyroid receptors during oligodendrocyte differentiation. Neuroreport. 1994; 5(14):1805–8. [PubMed: 7827337]
9. Apriletti JW, Ribeiro RC, Wagner RL, Feng W, Webb P, Kushner PJ, West BL, Nilsson S, Scanlan TS, Fletterick RJ, Baxter JD. Molecular and structural biology of thyroid hormone receptors. Clin Exp Pharmacol Physiol Suppl. 1998; 25:S2–11. [PubMed: 9809185]
10. Bhat MK, Parkison C, McPhie P, Liang CM, Cheng SY. Conformational changes of human beta 1 thyroid hormone receptor induced by binding of 3,3′,5-triiodo-L-thyronine. Biochem Biophys Res Commun. 1993; 195(1):385–92. [PubMed: 8363616]
11. Koenig RJ. Thyroid hormone receptor coactivators and corepressors. Thyroid. 1998; 8(8):703–13. [PubMed: 9737367]
12. Wagner RL, Apriletti JW, McGrath ME, West BL, Baxter JD, Fletterick RJ. A structural role for hormone in the thyroid hormone receptor. Nature. 1995; 378(6558):690–7. [PubMed: 7501015]
13. Darimont BD, Wagner RL, Apriletti JW, Stallcup MR, Kushner PJ, Baxter JD, Fletterick RJ, Yamamoto KR. Structure and specificity of nuclear receptor-coactivator interactions. Genes Devel. 1998; 12:3343–3356. [PubMed: 9808622]

14. Borngraeber S, Budny MJ, Chiellini G, Cunha-Lima ST, Togashi M, Webb P, Baxter JD, Scanlan TS, Fletterick RJ. Ligand selectivity by seeking hydrophobicity in thyroid hormone receptor. Proc Natl Acad Sci. 2003; 100(26):15358–63. [PubMed: 14673100]
15. Rodríguez-Fernández L, López-Jaramillo FJ, Bacher A, Fischer M, Weinkauf S. Improvement of the quality of lumazine synthase crystals by protein engineering. Acta Cryst. 2008; (F64):625–8.
16. Schwartz TU, Walczak R, Blobel G. Circular permutation as a tool to reduce surface entropy triggers crystallization of the signal recognition particle receptor-beta subunit. Protein Science. 2004; 13:2814–2818. [PubMed: 15340174]
17. Banatao D, Cascio D, Crowley C, Fleissner M, Tienson H, Yeates T. An approach to crystallizing proteins by synthetic symmetrization. Proc Natl Acad Sci U S A. 2006; 103(44):16230–5. [PubMed: 17050682]
18. Otwinowski Z, Minor W. Processing of x-ray diffraction data collected in oscillation mode. Methods Enzymol. 1997; 276:307–326.
19. Laskowski RA, MacArthur MW, Moss DS, Thornton JM. PROCHECK: a program to check the stereochemical quality of protein structures. J Appl Cryst. 1993; 26:283–291.
20. Mengeling BJ, Pan F, Privalsky ML. Novel mode of deoxyribonucleic acid recognition by thyroid hormone receptors: thyroid hormone receptor beta-isoforms can bind as trimers to natural response elements comprised of reiterated half-sites. Mol. Endocrinol. 2005; 19(1):35–51. [PubMed: 15459250]
21. Ribeiro RC, Feng W, Wagner RL, Costa CH, Pereira AC, Apriletti JW, Fletterick RJ, Baxter JD. Definition of the surface in the thyroid hormone receptor ligand binding domain for association as homodimers and heterodimers with retinoid X receptor. J Biol Chem. 2001; 276(18):14987–95. [PubMed: 11145963]
22. Togashi M, Nguyen P, Fletterick R, Baxter JD, Webb P. Rearrangements in thyroid hormone receptor charge clusters that stabilize bound 3,5′,5-triiodo-L-thyronine and inhibit homodimer formation. J Biol Chem. 2005; 280(27):25665–73. [PubMed: 15886199]
23. Bourguet W, Ruff M, Chambon P, Gronemeyer H, Moras D. Crystal structure of the ligand-binding domain of the human nuclear receptor RXR-alpha. Nature. 1995; 375:377–382. [PubMed: 7760929]
24. Brzozowski AM, Pike AC, Dauter Z, Hubbard RE, Bonn T, Engstrom O, Ohman L, Greene GL, Gustafsson JA, Carlquist M. Molecular basis of agonism and antagonism in the oestrogen receptor. Nature. 1997; 389:753–758. [PubMed: 9338790]
25. Pike AC, Brzozowski AM, Hubbard RE, Bonn T, Thorsell AG, Engstrom O, Ljunggren J, Gustafsson JA, Carlquist M. EMBO J. 1999; 18:4608–18. [PubMed: 10469641]
26. Grueninger D, Treiber N, Ziegler MO, Koetter JW, Schulze MS, Schulz GE. Designed protein-protein association. Science. 2008; 319(5860):206–9. [PubMed: 18187656]
27. Wukovitz SW, Yeates TO. Why protein crystals favour some space groups over others. Nat. Struct. Biol. 1995; 2:1062–7. [PubMed: 8846217]
28. Estébanez-Perpiñá E, Arnold LA, Jouravel N, Togashi M, Blethrow J, Mar E, Nguyen P, Phillips KJ, Baxter JD, Webb P, Guy RK, Fletterick RJ. Structural insight into the mode of action of a direct inhibitor of coregulator binding to the thyroid hormone receptor. Mol Endocrinol. 2007; (12):2919–28. [PubMed: 17823305]
29. Estébanez-Perpiñá E, Arnold LA, Nguyen P, Rodrigues ED, Mar E, Bateman R, Pallai P, Shokat KM, Baxter JD, Guy RK, Webb P, Fletterick RJ. A surface on the androgen receptor that allosterically regulates coactivator binding. Proc Natl Acad Sci. 2007; 104(41):16074–9. [PubMed: 17911242]

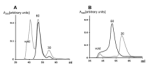

Fig. 1. Size exclusion chromatography of D355R TR LBD

Each protein peak is labeled with its apparent molecular mass (kDa). Panels (A) and (B) represent runs from independent protein preparations. (A) Initial run is shown in gray, rechromatographed fraction of dimeric TR is in black. (B) Protein was prepared in the presence (black line) or absence (gray line) of 50mM lithium sulfate.

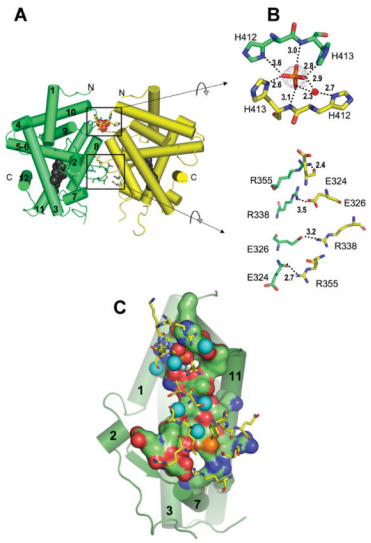

Figure 2. Structure of the TRβ D355R mutant dimer

(A) Cartoon representation of the dimer. The two TR monomers are shown in green (helixes are numbered) and yellow. The N- and C-termini of each LBD are labeled. Residues H412, H413, R355, E324, E326, R338 and sulfate ion at the dimer interface are shown as stick models and orange sphere, respectively. The bound hormone is shown as space-filling model in dark gray. The two boxed regions indicate the crucial polar interactions at the dimer interface (shown in detail on panel B).

(B) Network of contacting interfacial residues from two sites at the dimer interface. Residues are shown as stick models. Sulfate ion and water are drawn as stick model and sphere, respectively. Contacts between interacting residues and ions are indicated. The electron density corresponding to the sulfate ion (black mesh) in the 2Fo-Fc map is contoured at 2.0σ.

(C) Polar dimer interface. The intermolecular residues are in surface representation for the green monomer, and in stick representation for the yellow monomer. Shared at interface water molecules are depicted as cyan dotted spheres.

Figures were prepared with PyMOL from DeLano Scientific (http://www.pymol.org).

Table I

Data collection and refinement statistics

Crystallization	**TRβ Variant D355R**
Molecules per asymmetric unit	2
Space group	$P2_1$
Unit-cell dimensions a/b/c (Å) β (^{0})	55.5/92.9/58.8 110.0
Solvent content (%)	46.3
Matthews coefficient (Å^3/Da)	2.4
Resolution range, (Å)	25.0 –2.2
Number of unique reflections	28,544
Data redundancy	2.7 (1.9)[a]
Completeness (%)	90.2 (73.1)[a]
R_{symm} (%)	6.9
<I/σ(I)>	19.6 (3.0)[a]
R_{work} (%)/R_{free} (%)[b]	21.7/24.5
Rms deviation from ideality Bond length (Å) Bond angle (^{0})	0.008 1.19
Average B factor (A^2)	29.7

[a] numbers refer to the highest-resolution shell

[b] R_{work} /R_{free} = $\Sigma||F_o| - |F_c|| / \Sigma|F_o|$, where F_o and F_c are the observed and calculated structure factors, respectively. R_{free} is calculated for 5% of reflections randomly excluded from the refinement.

Table II
Contacting residues at the TR homodimer interface

Residues in this table have at least one atom within 4.0Å of an atom in the partner molecule of the dimer.

Residue in Chain A	Residue in Chain B
Tyr^{321}	Met^{358}
Pro^{323}	Met^{358}
Glu^{324}	Arg^{355}
Glu^{326}	Met^{358}
Arg^{338}	Glu^{326}
Arg^{355}	Glu^{324}
Met^{358}	Tyr^{321}
Met^{358}	Pro^{323}
Met^{358}	Glu^{326}
Ser^{359}	Pro^{323}
Ser^{361}	Ser^{361}
Ser^{361}	Ser^{362}
Ser^{362}	Ser^{361}
Ser^{362}	Asn^{364}
Asn^{364}	Ser^{362}
Asn^{364}	Asn^{364}
Asn^{364}	His^{413}
Asn^{364}	Val^{414}
Arg^{410}	His^{413}
His^{412}	His^{413}
His^{413}	Asn^{364}
His^{413}	Arg^{410}
His^{413}	His^{412}
Val^{414}	Asn^{364}